BASIC–LIVER, PANCREAS, AND BILIARY TRACT

Targeted Deletion of FATP5 Reveals Multiple Functions in Liver Metabolism: Alterations in Hepatic Lipid Homeostasis

HOLGER DOEGE,* REBECCA A. BAILLIE,† ANGELICA M. ORTEGON,§ BERNICE TSANG,§ QIWEI WU,* SANDHYA PUNREDDY,¶ DAVID HIRSCH,‖ NICKI WATSON,‖ RUTH E. GIMENO,¶ and ANDREAS STAHL*,§

*Division of GI/Hepatology, Stanford University School of Medicine, Stanford, California; †Lipomics Technologies, Inc, West Sacramento, California; §Palo Alto Medical Foundation Research Institute, Palo Alto, California; ¶Millennium Pharmaceuticals, Inc, Cambridge, Massachusetts; and ‖Whitehead Institute for Biomedical Research, Cambridge, Massachusetts

Background & Aims: **Fatty acid transport protein 5 (FATP5/Slc27a5) has been shown to be a multifunctional protein that in vitro increases both uptake of fluorescently labeled long-chain fatty acid (LCFA) analogues and bile acid/coenzyme A ligase activity on overexpression. The aim of this study was to further investigate the diverse roles of FATP5 in vivo.** ***Methods:*** **We studied FATP5 expression and localization in liver of C57BL/6 mice in detail. Furthermore, we created a FATP5 knockout mouse model and characterized changes in hepatic lipid metabolism (this report) and bile metabolism (the accompanying report by Hubbard et al).** ***Results:*** **FATP5 is exclusively expressed by the liver and localized to the basal plasma membrane of hepatocytes, congruent with a role in LCFA uptake from the circulation. Overexpression of FATP5 in mammalian cells increased the uptake of ^{14}C-oleate. Conversely, FATP5 deletion significantly reduced LCFA uptake by hepatocytes isolated from FATP5 knockout animals. Moreover, FATP5 deletion resulted in lower hepatic triglyceride and free fatty acid content despite increased expression of fatty acid synthetase and also caused a redistribution of lipids from liver to other LCFA-metabolizing tissues. Detailed analysis of the hepatic lipom of FATP5 knockout livers showed quantitative and qualitative alterations in line with a decreased uptake of dietary LCFAs and increased de novo synthesis.** ***Conclusions:*** **Our findings support the hypothesis that efficient hepatocellular uptake of LCFAs, and thus liver lipid homeostasis in general, is largely a protein-mediated process requiring FATP5. These new insights into the physiological role of FATP5 should lead to an improved understanding of liver function and disease.**

Maintaining appropriate long-chain fatty acid (LCFA) uptake by the liver is crucial for energy homeostasis. During starvation, LCFAs are mobilized from adipose tissue, taken up by the liver, and converted into ketone bodies and other substrates. Disruption of these processes, as found in some hereditary defects of liver LCFA uptake, is associated with acute liver failure and mortality.[1,2] The underlying genetic defect(s), however, are currently unknown. Conversely, excessive liver LCFA uptake (eg, due to visceral adiposity and elevated portal fatty acid [FA] levels)[3] is associated with insulin desensitization, type 2 diabetes mellitus,[4] and nonalcoholic fatty liver disease.[5] Considerable evidence has accumulated that in addition to diffusion, LCFA uptake by the liver,[6–11] intestine,[12–14] heart,[10,15] adipose tissue,[16] and other organs is mediated by a saturable and specific LCFA transport system.[17,18] Investigators have found several membrane proteins that, when overexpressed in cultured mammalian cells, increase the uptake of LCFAs. The most prominent and best characterized of these are FAT/CD36 and fatty acid transport proteins (FATPs, solute carrier family 27) 1 or 4. However, neither CD36[19,20] nor FATP1 or FATP4[13,16,18,21] is expressed at appreciable levels in the liver. Furthermore, CD36-null animals show reduced LCFA uptake into skeletal muscle and heart but increased uptake by the liver.[22–24]

Based on sequence analyses, we have previously found that FATP5 is a member of the *FATP* gene family[21,25] and that FATP5, like the other members of the FATP family, can enhance the uptake of BODIPY-FA upon transient overexpression in HEK293 cells.[21] In addition

Abbreviations used in this paper: FA, fatty acid; FACS, fluorescence-activated cell sorter; FAS, fatty acid synthetase; FATP, fatty acid transport protein; FFA, free fatty acid; HBS, Hank's buffered salt solution; LCFA, long-chain fatty acid; PCR, polymerase chain reaction; TG, triglyceride.

0016-5085/06/$32.00
doi:10.1053/j.gastro.2006.02.006

to its function as FA transporter, FATP5 also facilitates at least 2 different enzymatic reactions. As is the case for FATP1, FATP2, and FATP4,[26–28] FATP5 can activate LCFAs and very long-chain fatty acids by catalyzing the covalent attachment of coenzyme A (CoA).[28] Furthermore, FATP5 is also involved in the reactivation, but not de novo synthesis, of C24 bile acids to their CoA derivatives.[29,30] However, how these functions are integrated in vivo is only poorly understood. To this end, we investigated localization of FATP5 in vivo and created a FATP5 knockout mouse model to study its contribution to bile (Hubbard et al[31]) and lipid metabolism (this report). Here we show that FATP5 is a liver-specific protein required for efficient hepatic LCFA uptake and hepatic lipid homeostasis.

Materials and Methods

Materials

Deoxycitidine-5′[α-^{32}P]triphosphate and Tri-[9,10-^{3}H(N)]oleoylglycerol (^{14}C-triolein) were purchased from Amersham Bioscience (Piscataway, NJ). ^{14}C-oleate, ^{14}C-taurocholate, 4,4-difluoro-5-methyl-4-bora-3a,4a-diaza-s-indacene-3-dodecanoid acid (C1-BODIPY-C12), and cerulenin were obtained from ARC Inc (St Louis, MO), Molecular Probes (Eugene, OR), and Alexis Biochemicals (San Diego, CA), respectively. All other chemicals were obtained from Sigma Chemical Co (St Louis, MO).

Antibodies

Murine FATP5 specific antibody was raised in rabbits against a glutathione *S*-transferase/FATP5 fusion protein. The FATP5 portion of the fusion protein was comprised of the last 93 C-terminal amino acids of FATP5. Monoclonal antibodies against murine fatty acid synthetase (FAS), CD31, and β-catenin were purchased from BD Bioscience (Palo Alto, CA), Jackson ImmunoResearch (West Grove, PA), and Transduction Labs (Lexington, KY), respectively. The antibody against murine keratin 8 was obtained from the Developmental Studies Hybridoma Bank (Iowa City, IA).

Animal Experiments

Animals were maintained on regular laboratory chow (5P75; LabDiet, Richmond, IN). Triglyceride (TG), cholesterol, bile acid, albumin (all from Sigma Diagnostics, St Louis, MO), free fatty acid (FFA; Wako Chemicals, Richmond, VA), alanine aminotransferase, bilirubin (Stanbio Laboratory, Boerne, TX), and insulin (ALPCO Diagnostics, Windham, NH) levels were determined using commercial kits. All animal experiments were approved by the Institutional Animal Care and Use Committee of Palo Alto Medical Foundation Research Institute.

Generation of FATP5 Knockout Mice

Genomic DNA containing the FATP5 locus was identified by screening a 129Sv genomic bacterial artificial chromosome library with a fragment containing the 5′ end of the FATP5 coding sequence. Polymerase chain reaction (PCR) primers were designed to amplify a 6.2-kilobase fragment of genomic DNA upstream of the initiation codon (5′ arm) and a 2.1-kilobase fragment downstream of the first exon (3′ arm). The amplified arms were subcloned into a targeting vector containing a neomycin resistance marker under control of the PGK promoter and a promoter-less *lacZ* gene with a nuclear localization sequence located downstream of the 5′ arm. 129Sv embryonic stem cells were electroporated with the targeting construct and screened by Southern blotting. Embryonic stem cell clones that had undergone homologous recombination were injected into blastocysts. Injected blastocysts were transferred into pseudopregnant mice to generate chimeric offspring. Male chimeras were mated with C57BL/6 female mice. Genotyping of offspring was performed by PCR.

Northern Blots

Northern blots were obtained from Clontech (Palo Alto, CA) and hybridized with ^{32}P-labeled cDNA probes for human FATP5 generated by PCR (primer pair: hF5pfw, 5′-tcttgcaacaggttaacgtg-3′/hF5prv, 5′-gggctagctgcacagcagcca-3′) as previously described.[21]

Hepatic TG Secretion

After a fasting period of 4 hours, anesthetized mice were injected intravenously with Triton WR 1339 diluted in saline (200 mg/mL) via the tail vein (500 mg/kg body wt).[32] Blood samples were taken before the injection (t = 0) and 60, 120, and 210 minutes after injection and serum TG levels determined.

Hepatic Lipase Activity

Enzyme activity was assayed using a method described by Nilsson-Ehle and Schotz.[33]

^{14}C-Lipid Gavage

Mice were given an intragastric 200 μL olive oil bolus containing 2 μCi ^{14}C-oleic acid. Before (t = 0) and at 30, 60, 120, and 240 minutes after administration, blood samples (75 μL) were taken by orbital eye bleeding and tissues were harvested after the last time point. ^{14}C-content was measured by scintillation counting and normalized to milligram protein content for tissues.

Inhibition of FA de novo Synthesis

Mice were injected intraperitoneally with cerulenin 60 $mg \cdot kg^{-1} \cdot day^{-1}$ for 3 days and kept under absence of food with access to water ad libitum. After 56 hours, animals were sacrificed and their livers were harvested.

Hepatocyte Preparation and Fluorescence-Activated Cell Sorter Analysis

Mouse livers were cannulated through the portal vein, and an incision was made in the inferior vena cave. Liver perfusion with digestion and perfusion media and isolation of hepatocytes were performed according to the manufacturer's instructions (Gibco, Carlsbad, CA). After isolation, hepatocytes were resuspended in HepatoZYME (Gibco) containing 0.1% FA-free bovine serum albumin (Sigma Diagnostics). C1-BODIPY-C12/bovine serum albumin solution[13] was added to the hepatocytes to yield final concentrations of 2 μmol/L or 0.1%, respectively. Uptake at 37°C was stopped after the indicated time points by transferring 100 μL of the cells into 5 mL of ice-cold stop solution (Hank's buffered salt solution [HBS], 0.1% bovine serum albumin). Cells were pelleted by centrifugation and resuspended in 250 μL cold fluorescence-activated cell sorter (FACS) buffer (HBS containing 20 mmol/L EDTA, 10% fetal calf serum, and 1 μg/mL propidium iodine). Mean BODIPY uptake by living cells (propidium iodine negative, dead cells gated out) was determined using a FACSCalibur (Becton Dickinson, Rockville, MD).

Tissue Lipid Analysis

Tissue samples were powdered in liquid nitrogen, total lipids were extracted by the method of Folch et al,[34] and TG content was measured.

FA Uptake Measurement in Hepatocytes Using ^{14}C-Labeled Oleate

Alternatively, LCFA uptake by isolated hepatocytes was assayed using ^{14}C-oleate essentially as previously described.[35,36] Briefly, isolated hepatocytes were allowed to attach overnight to a type I collagen–coated 12-well cluster plate. Dead cells were removed by 2 washes with serum-free HepatoZYME and incubated at 37°C for 15 seconds with a prewarmed uptake solution containing 200 μmol/L ^{14}C-oleate bound to bovine serum albumin at a 2:1 molar ratio in HBS resulting in an approximate unbound oleate concentration of 400 nmol/L. Wells were washed twice with ice-cold stop solution and cells were lysed in 200 μL radioimmunoprecipitation assay buffer (150 mmol/L NaCl, 1% Nonidet P-40, 0.5% deoxycholic acid, 0.1% sodium dodecyl sulfate, 50 mmol/L Tris, pH 8.0) for 30 minutes on ice. A total of 150 μL of lysate was subsequently used for scintillation counting, and 30 μL was used for colorimetric protein determination (Pierce, Rockford, IL).

FA Uptake Measurement in HeLa Cells

HeLa cell monolayers were transiently transfected with the indicated constructs or with empty vector (pcDNA3.1) using FuGENE reagent (Roche, Palo Alto, CA). Two days after transfection, cells were detached, counted, washed with HBS, and incubated at 37°C for the indicated time points with uptake solution containing either 1 μmol/L ^{14}C-oleate or ^{14}C-taurocholate and 0.1% bovine serum albumin in HBS in the absence or presence of 50 μmol/L unlabeled taurocholate. The reaction was stopped with ice-cold stop solution. Cells were transferred onto Whatman paper using an automatic harvester (Brandel, Gaithersburg, MD), washed 3 times with stop solution, and subsequently used for scintillation counting.

Immunofluorescence and Immunoelectron Microscopy

Immunofluorescence[37] and immunoelectron microscopy[13] were performed as described before.

Lipid Analysis

The lipids from plasma (200 μL) and tissues (25 mg) were extracted in the presence of authentic internal standards.[34] Individual lipid classes within each extract were separated by preparative thin-layer chromatography as described previously.[38] Isolated lipid classes were trans-esterified in 3N methanolic HCl in a sealed vial under a nitrogen atmosphere at 100°C for 45 minutes. The resulting FA methyl esters were extracted from the mixture with hexane containing 0.05% butylated hydroxytoluene and prepared for gas chromatography by sealing the hexane extracts under nitrogen. FA methyl esters were separated and quantified by capillary gas chromatography using a gas chromatograph (model 6890; Hewlett-Packard, Wilmington, DE) equipped with a 30-m DB-225MS capillary column (J&W Scientific, Folsom, CA) and a flame-ionization detector as described previously.[38] Liver lipid metabolite data were displayed using the Lipomics Surveyor visualization software (Lipomics Tech. Inc., Sacramento, CA), which illustrates the quantitative differences in concentration of each lipid metabolite when comparing wild-type and FATP5 knockout mice. Column headings display the FA and families of FAs present in each lipid class listed in the row headings. Surveyor's heat map display is read as follows: each square represents the statistical comparison of the difference in concentration of a single FA. A higher concentration of a specific metabolite is displayed in green, whereas a lower concentration is displayed in red. The brightness of the color indicates the magnitude of the difference as detailed in the legend. Mean differences not meeting $P < .05$ (assessed by Student t test) are displayed in black.

Statistics

Chemiluminescent signals were directly quantified using Kodak 1D version 3.5.3 software (Kodak, Rochester, NY). The absolute integration value of the immunoreactive bands minus background was determined. Statistical analysis was determined by nonpaired Student t test.

Results

FATP5 Is Specifically Expressed in Liver

Based on our initial observation that FATP5 is expressed in liver but not in heart, brain, spleen, lung, muscle, kidney, or testis,[21] we expanded Northern blot

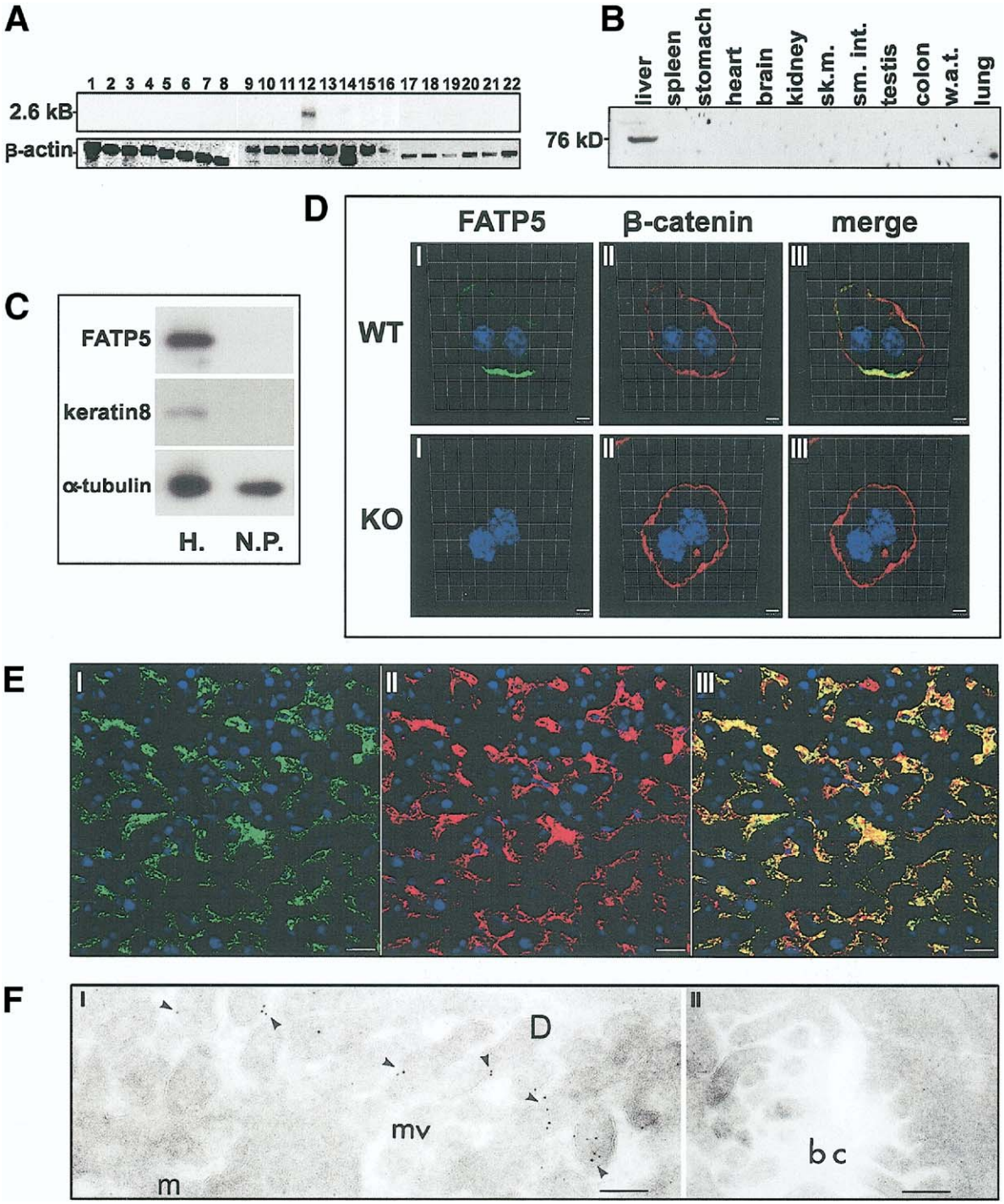

Figure 1. Expression of FATP5 in the liver. (*A*) Analysis of FATP5 messenger RNA expression in human tissues. Commercially available Northern blots were hybridized with a human FATP5 complementary DNA radiolabeled by random priming. 1, peripheral blood lymphocytes; 2, colon; 3, small intestine; 4, ovary; 5, testis; 6, prostate; 7, thymus; 8, spleen; 9, pancreas; 10, kidney; 11, skeletal muscle; 12, liver; 13, lung; 14, placenta; 15, brain; 16, heart; 17, fetal liver; 18, bone marrow; 19, tonsil; 20, thymus; 21, lymph node; 22, spleen. (*B*) Western blot analysis of FATP5 expression. Protein lysates of the indicated mouse tissues were prepared as described in Materials and Methods. Equal amounts of lysates were separated by reducing sodium dodecyl sulfate/polyacrylamide gel electrophoresis and transferred onto nitrocellulose. Mouse FATP5 protein was immunochemically detected with a specific antiserum against its last 93 C-terminal amino acids. (*C*) Western blot analysis of FATP5 expression in mouse hepatocytes (H.)/nonparenchymal cells (N.P.) separated by differential centrifugation. The keratin-8 control was used as hepatocyte-specific marker. α-Tubulin was loading control. (*D*) Confocal microscopic analysis of mouse FATP5 in an isolated hepatocyte. Hepatocytes of wild-type (WT) or FATP5 knockout (KO) mice stained for FATP5 (fluorescein isothiocyanate, *green*) and β-catenin (Cy3, *red*) as plasma membrane marker. *Blue*, 4′,6-diamidino-2-phenylindole–stained cell nuclei (*scale bars* = 4 μm). (*E*) Three-dimensional reconstruction of FATP5 protein (I, *green*) and endothelial cell marker CD31 (II, *red*) specific immunofluorescence in mouse liver from confocal image stacks (III, overlap of both channels) (*scale bar* = 17 μm). (*F*) Immunoelectron microscopy of mouse liver sections. Specific FATP5 immunogold labeling of space of Disse (I) and bile canaliculi (II). *Arrowheads* indicate position of gold particles. D, space of Disse; mv, microvilli; m, mitochondria; bc, bile canaliculus (*scale bars* = 0.20 μm).

analyses and performed an extended survey of FATP5 messenger RNA expression in 21 human tissues, including fetal liver. As shown in Figure 1*A*, FATP5 messenger RNA was detected in mature liver but was absent in fetal liver, which is primarily a hematopoietic organ. In all other tissues investigated, no signal was found. To ascertain these findings with a second, independent method and to analyze the tissue distribution of FATP5 protein, protein lysates of various mouse tissues were separated by sodium dodecyl sulfate/polyacrylamide gel electrophoresis and probed with a novel FATP5-specific antiserum. In accordance with the predicted molecular weight of 76 kilodaltons, a specific immunoreactive band was detected exclusively in the liver lysate (Figure 1*B*). Additionally, after separating the hepatocyte from the nonparenchymal cell fraction by differential centrifugation, we could show that FATP5 is predominantly expressed by hepatocytes (Figure 1*C*).

FATP5 Is Localized to the Space of Disse

To further study the subcellular localization of FATP5 protein, we performed immunofluorescent microscopy of both isolated mouse hepatocytes and mouse liver sections. Confocal microscopy showed that FATP5 protein was largely localized to the plasma membrane of hepatocytes, as revealed by costaining with the membrane marker β-catenin (Figure 1*D*). The preferred plasma membrane localization was also apparent in 3-dimensional restoration analyses of single hepatocytes (Supplementary Figure 1; see supplemental material online at http://www.pamf.org/research/stahl/resources/gastro2686). As expected, no immunofluorescent signal for FATP5 was found in the FATP5 knockout hepatocytes, further demonstrating the specificity of the FATP5 antiserum (Figure 1*D*). Three-dimensional reconstruction of confocal sections through fresh frozen mouse liver showed a branching, tubular distribution of FATP5 protein throughout the liver (Figure 1*E*). We used CD31 as a marker to identify hepatic sinusoidal endothelial cells.[39] Costaining of FATP5 and CD31 showed that these tubular structures coincided with the liver sinusoids (Figure 1*E*). To confirm this highly restricted localization pattern, we performed immunoelectron microscopy studies of frozen liver sections. Hepatocytes are polarized cells with apical plasma membranes forming specializations that constitute bile canaliculae and basal plasma membranes that form, together with the fenestrated sinusoidal endothelial cells, the space of Disse. Both spaces are densely populated by hepatic microvilli. Interestingly, FATP5 was predominantly localized to microvilli in the space of Disse and underlying membrane structures, while the protein was completely absent from apical villi (Figure 1*F*).

Targeted Deletion of FATP5 Results in Viable FATP5 Knockout Mice

The murine FATP5 gene is located on mouse chromosome 7 spanning over 10 coding exons (Figure 2*A*). Homologous recombination was used to replace the first exon with a cassette containing a selectable marker and a *lacZ* gene, which results in a deletion of the first 228 amino acids of the FATP5 protein. The correct recombination event was confirmed both by PCR (Figure 2*C*) and Southern blotting with probes specific for the 5′ and 3′ arm (Figure 2*B*), respectively. FATP5 knockout mice were obtained at Mendelian ratios from heterozygous mating pairs and were fertile. Animals homozygous for the FATP5 deletion allele lacked any detectable FATP5 in liver (Figure 2*D*, fifth column). FATP5 knockout mice appeared to be indistinguishable from wild-type littermates and when fed a standard laboratory chow diet had similar body weight and length.

Next, we investigated which of the other FATP protein family members besides FATP5 are expressed in liver and whether their expression would be altered as a result of the FATP5 deletion. To that end, equal amounts of liver lysates from wild-type or FATP5 knockout mice were analyzed with antisera specific for each of the 6 FATP isoforms. In the lysates from wild-type animals, specific bands for FATP2 and FATP5 were clearly detected, as well as a weak expression of FATP3 and FATP4 (Figure 2*D*, upper row). Lysates from tissues known to be positive for the expression of FATP1 (adipose tissue), FATP4 (jejunum), and FATP6 (heart) were used to verify that liver expression of these genes was very weak or nondetectable (Figure 2*D*, lower row). Lysates from FATP5 knockout animals showed no compensatory up-regulation of FATP1–4 or FATP6 in the livers (Figure 2*D*, middle row).

FATP5 Knockout Hepatocytes Have Reduced FA Uptake

Initial FACS analyses showed a clear difference in the physical parameters of wild-type and FATP5 knockout hepatocytes from ad libitum–fed animals. Forward scatter, a measurement of cell size, was increased, while side scatter, a measurement of cellular granulosity, was decreased for FATP5 knockout hepatocytes (Figure 3*A*). The observed shift in forward scatter indicates a slight hepatocyte hypertrophy in FATP5 knockout livers, which was also noticed in H&E-stained liver sections (average hepatocyte diameters, 18.7 μm vs 15.1 μm) and is in line with the observed trend toward a hepatomegaly in FATP5 knockout mice (Hubbard

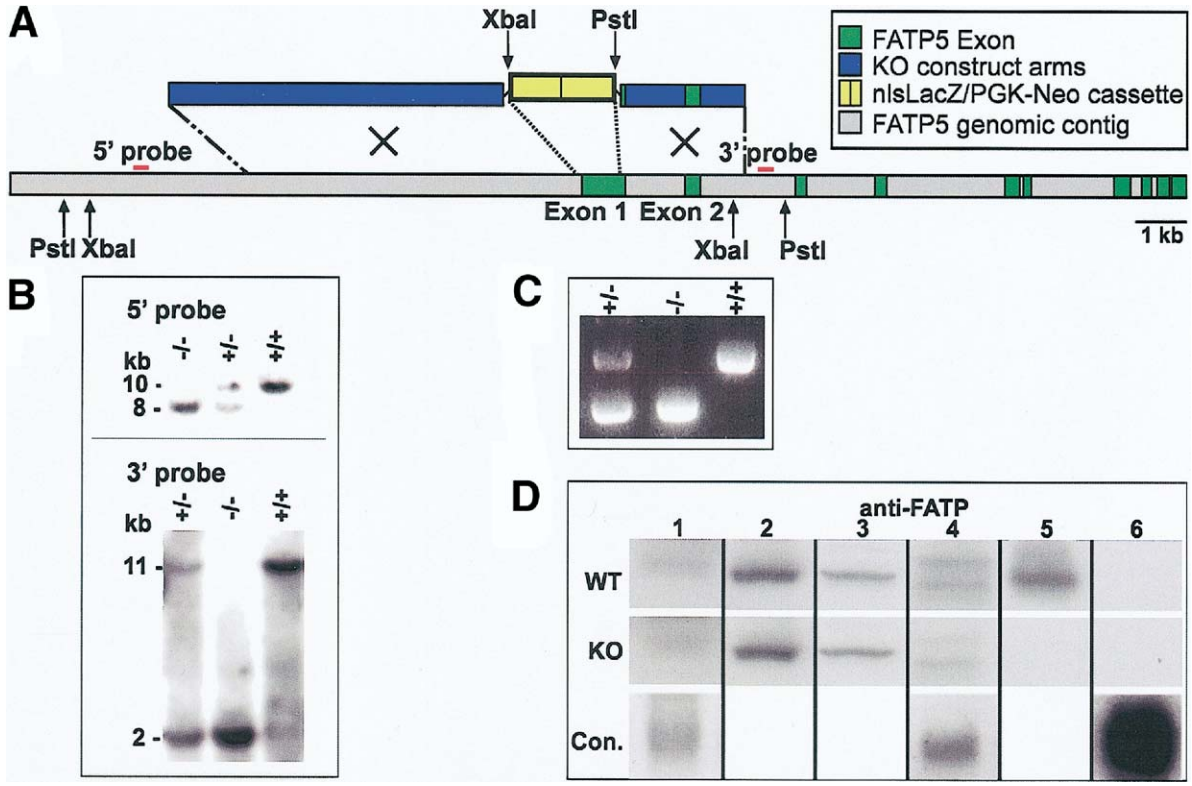

Figure 2. Generation of FATP5 knockout mice. (*A*) Map of the FATP5 genomic locus and the targeting construct. (*B*) Southern blot using genomic DNA from the tail of F2 animals digested with *Xba*I and *Pst*I, respectively, and hybridized with the 5′ and 3′ probes. (*C*) PCR detection of altered FATP5 locus from genomic DNA. (*D*) Western blot analysis of wild-type (WT) and FATP5 knockout (KO) liver lysates using antisera specific for FATP1–6. Con., positive control tissue (FATP1, adipocytes; FATP4, jejunum; FATP6, heart). Rows show same amount of protein lysate from FATP5 KO and WT animals run side by side on the same blot.

et al[31]). Because the change in side scatter could indicate a lower abundance of intracellular lipid droplets, we quantified neutral lipids by FACS-analyzed Nile red–stained hepatocytes. Significantly lower values for the FATP5 knockout versus wild-type hepatocytes (190 vs 271) were observed (Figure 3*B*).

To test if the decreased hepatocellular lipid content is a direct result of impaired hepatocellular LCFA uptake due to the loss of FATP5, we established two independent LCFA uptake assays using freshly isolated hepatocytes from ad libitum–fed FATP5 knockout and wild-type mice. Initially, short-term (30-second) LCFA uptake was determined using the fluorescently labeled FA analogue C1-BODIPY-C12. This FACS-based assay showed that LCFA uptake by FATP5 knockout hepatocytes was uniformly decreased by >40% (Figure 3*C* and *D*). Uptake over shorter and longer periods was also significantly reduced in FATP5 knockout cells (Figure 3*D*). Secondly, we measured uptake of ^{14}C-radiolabeled oleic acid by isolated hepatocytes. As shown in Figure 3*E*, LCFA uptake was reduced by nearly 50%, which is in line with the results collected from the FACS-based measurements.

Overexpression of FATP5 in Cultured Mammalian Cells Increases Uptake of FAs but not of Bile Acids

Because FATP5 is also involved in bile acid metabolism, as described in the accompanying report by Hubbard et al,[31] we wanted to compare its transport function with a bona fide bile transporter, SLC10A1.[40,41] As shown in Figure 3*F* and *G*, overexpression of FATP5, but not of SLC10A1, resulted in a rapid increase of oleate uptake (Figure 3*F*). Oleate uptake could not be competed with a 50-fold excess of unlabeled taurocholate (Figure 3*F*). Under the same assay conditions, SLC10A1 showed a robust and significant increase in ^{14}C-taurocholate uptake compared with the vector control, which was not observed in the FATP5-overexpressing cells (Figure 3*G*).

FATP5 Knockout Livers Have Decreased Lipid Content and Altered Lipid Profiles

Initial assessment of liver composition showed that total diglyceride and TG content was reduced by 48% (data not shown). To determine changes in hepatic liver compo-

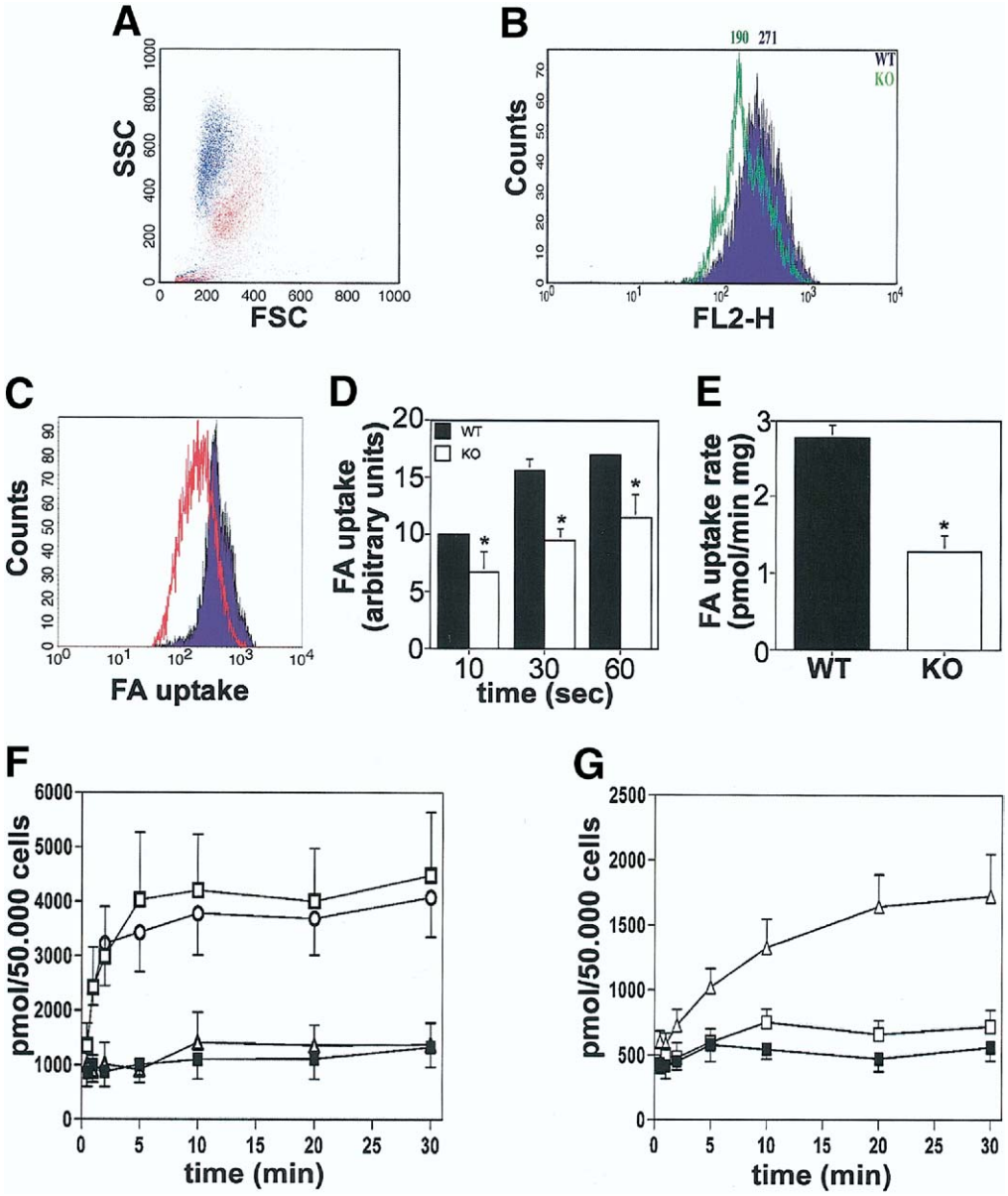

Figure 3. Impaired FFA uptake of FATP5 knockout hepatocytes. (*A*) FACS analysis of wild-type (*blue*) and FATP5 knockout (*red*) hepatocytes. FSC, forward scatter; SSC, side scatter. (*B*) Quantification of Nile red–stained hepatocytes of wild-type (*blue*) and FATP5 knockout (*green*) hepatocytes by FACS analysis. (*C*) Histogram plot of wild-type (*blue*) and FATP5 knockout (*red*) hepatocytes after 30-second incubation with C1-BODIPY-C12. (*D*) Mean fluorescence of FATP5 wild-type (*black bars*) and knockout (*white bars*) hepatocyte populations after 10-, 30-, and 60-second incubation with C1-BODIPY-C12. (*E*) Uptake of ^{14}C-radiolabeled oleic acid by hepatocytes of wild-type (*black bar*) and FATP5 knockout (*white bar*) animals. (*F*) Uptake of ^{14}C-radiolabeled oleic or (*G*) taurocholic acid by HeLa cells overexpressing FATP5 (*white circles*), FATP5 in the presence of 50-fold unlabeled taurocholate (*white squares*), and SLC10A1 (*white triangles*). *Black squares*, empty vector control. (*E–G*) The graphs represent means ± SEM of data from 3 independent experiments, each assayed in triplicate. $*P <$ .05 in *t* test. No significance between FATP5 and vector control in *G*.

sition in further detail, we performed gas chromatography/mass spectrometry–based analyses of wild-type and FATP5 knockout liver lysates as detailed in Materials and Methods. Using this technique, we found that total TG levels were reduced by 59% in FATP5 knockout livers compared with wild-type littermates (Figure 4*A*). Compositional analysis showed a disproportional decrease in saturated (62%) and polyunsaturated FAs (60%) compared with monounsaturated FAs (55%). Total intracellular FFA levels were decreased by 37% (Figure 4*B*). Interestingly, the degree of lipid reduction in FATP5 knockout livers was similar to the decrease in LCFA uptake by isolated FATP5 knockout hepatocytes (Figure 3*D* and *E*). The reduction in saturated FAs (41%) was more pronounced than the decrease in monounsaturated (31%) and polyunsaturated (30%) FAs (Figure 4*B*). Amounts of cholesterol esters were likewise reduced, probably as a direct result of this decline in intracellular FA levels (Figure 4*C*).

Because FATP5 has been reported to possess very-long-chain acyl-CoA synthetase activity, we compared a comprehensive analysis of FA classes and chain lengths from livers of FATP5 knockout animals with that of wild-type littermates. No change in chain length distribution was detected in any of the 10 lipid classes analyzed (Figure 4*D*). Total phospholipid mass in liver of FATP5 knockout animals was slightly lower than in wild-type animals. Interestingly, phosphatidylserine concentrations were significantly higher (9044 ± 3130 vs 5739 ± 485 nmol/g) in FATP5 knockout livers, whereas cardiolipin and phosphatidylcholine showed an obvious trend toward lower concentrations.

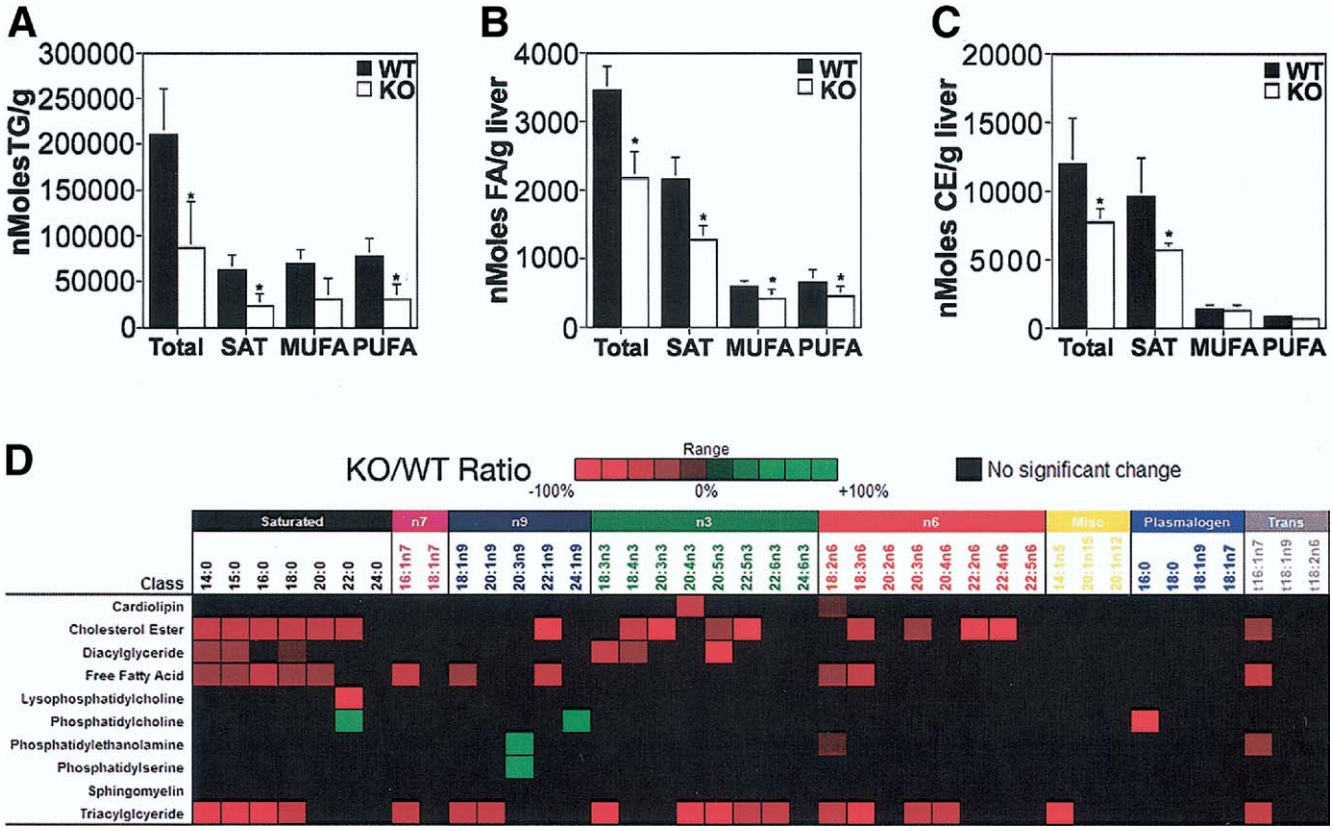

Figure 4. Changes in FATP5 knockout liver lipid composition. (*A*) Liver TG content. (*B*) Liver FFA content. (*C*) Liver cholesterol ester (CE) content. SAT, saturated fatty acids; MUFA, monounsaturated fatty acids; PUFA, polyunsaturated fatty acids. (*D*) Lipomics Surveyor heat map comparing the lipid composition of wild-type and FATP5 knockout liver samples as described in Materials and Methods. All experiments were performed with 2 cohorts of 6 female animals. Similar results were obtained using male animals. $*P < .05$ in *t* test.

FATP5 Knockout Livers Have Altered Hepatic Lipid Distribution and Increased de novo FA Synthesis

To assess whether the observed qualitative and quantitative alterations in hepatic lipid composition in FATP5 knockout mice would be reflected by a difference in lipid deposition throughout the liver, we investigated hepatic lipid distribution by Oil Red O staining of liver sections. In regard to its metabolic function, the liver acinus is divided into 3 zones based on distance from the feeding vessels and oxygen supply. Glucose-liberating and FA-oxidizing enzymes are predominantly expressed in zone 1, whereas glycolytic and FA-synthesizing enzymes are preferentially expressed in zone 3.[42]

Although H&E staining has shown no significant structural alterations between FATP5 knockout and wild-type mice (data not shown), we found clear differences in staining of neutral lipids (Figure 5*A*). Wild-type animals fed ad libitum showed neutral lipid accumulation, preferentially around the hepatic triads, which reflects the known nutrient and gene expression gradients within the liver. Staining of neutral lipids in the FATP5 knockout liver was weaker and diffuse between the individual liver zones (Figure 5*A*, upper panel). To increase hepatic TG uptake, we used a 48-hour fast. Livers from starved wild-type mice showed a robust Oil Red O staining and demonstrated an even neutral lipid distribution throughout the liver. In contrast, livers of FATP5 knockout animals showed a patchy Oil Red O staining pattern. Strong neutral lipid accumulation could be detected particularly around central veins but was greatly reduced or absent from other areas (Figure 5*A*, lower panel). These results suggest that a large amount of the lipids in the FATP5 knockout liver are the product of de novo biosynthesis rather than imported from the circulation. This notion was supported by our finding that FAS expression was greatly increased in FATP5 knockout livers (Figure 5*B*). To compare the contribution of de novo lipid synthesis with liver TG content, we treated mice with the FAS inhibitor cerulenin.[43,44] As shown in Figure 5*C*, the decrease in liver TG content after cerulenin treatment relative to mock treatment showed a clear trend to be more pronounced in the FATP5 knockout animals compared with the wild-type littermates, pointing to a more essential role of LCFA de

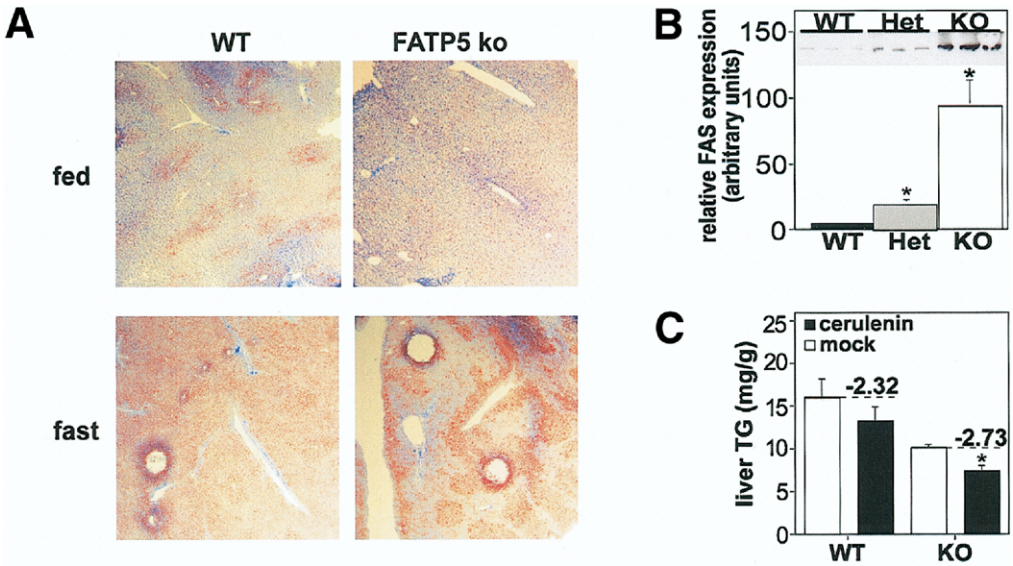

Figure 5. Altered lipid accumulation and increased FAS expression in the FATP5 knockout liver. (*A*) Neutral lipids in wild-type (WT) and FATP5 knockout mouse (KO) livers were visualized by Oil Red O/hematoxylin staining of mice fed ad libitum (*upper panel*) or after a 48-hour fasting period (*lower panel*) of the animals. (*B*) Western blot analysis of FAS expression in liver lysates from wild-type (WT), FATP5 heterozygote (Het), and FATP5 knockout (KO) mice. Densitometric quantification is shown in the lower panel. $*P < .05$ in *t* test. (*C*) Effect of FAS inhibition on liver TG content after a 56-hour fasting period. Wild-type and FATP5 knockout mice were treated with the FAS inhibitor cerulenin (*black bars*) or mock (*white bars*) as described in Materials and Methods. $*P < .05$ in *t* test.

novo synthesis in livers of FATP5 knockout animals, underlining our results gained from the hepatic FAS expression analysis.

FATP5 Deletion Results in Decreased Hepatic TG and Ketone Body Output in the Fasting State

To test whether the observed reduction in hepatic TG and cholesterol ester stores would also result in decreased hepatic lipoprotein secretion, we injected the lipase inhibitor Triton WR 1339 into both FATP5 knockout mice and wild-type littermates after a 4-hour fast and studied serum TG levels. Strikingly, FATP5 knockout animals showed greatly impaired liver TG secretion, particularly at later points of the Triton WR 1339 treatment (Figure 6*A*), whereas initial hepatic lipase expression (data not shown) and activity (6.1 ± 0.51 vs 6.4 ± 0.65) mol/(mL · h · e^{12}) as well as serum TG levels, were comparable between FATP5 knockout mice and wild-type littermates. Next, we measured hepatic ketone body production under fasting conditions. To that end, we performed an oil gavage to initially administer both FAP5 knockout and wild-type animals equal amounts of lipids. We subsequently assayed the concentrations of serum β-hydroxybutyrate, one of the predominant ketone bodies produced by the liver, during a 48-hour starvation period. For shorter fasting periods (0–24 hours), we found a trend toward decreased β-hydroxybutyrate levels that became more dramatic at later points (Figure 6*B*). This observation demonstrated a significantly impaired ketogenetic response to fasting in the FATP5 knockout animals. In summary, our findings gained from these experiments show a profoundly impaired liver metabolite output that is likely a direct result of the reduced hepatic lipid stores.

FATP5 Deletion Results in Impaired Serum Clearance and Deposition in the Postprandial State

To investigate whether the impaired hepatic LCFA uptake capacity and lipid content would be reflected by alterations in lipid absorption or deposition, we next measured clearance of lipids in FATP5 knockout and wild-type animals in the postprandial state. To that end, we performed oil gavages after an overnight fast and subsequently measured serum FFA and TG levels. As shown in Figure 6*C* and *D*, wild-type mice showed a peak in FFA concentrations after 30 minutes (1.51 mmol/L) and in TG concentrations after 60 minutes (182 mg/dL). In the FATP5 knockout mice, the increase was more pronounced (2.25 mmol/L for FFA, 411 mg/dL for TG) and persisted longer. Taken together, these results indicate an impairment in FFA and TG clearance from circulation in the postabsorptive state after FATP5 deletion but also point to a normal absorption of dietary lipids in intestine as observed by Hubbard et al.[31]

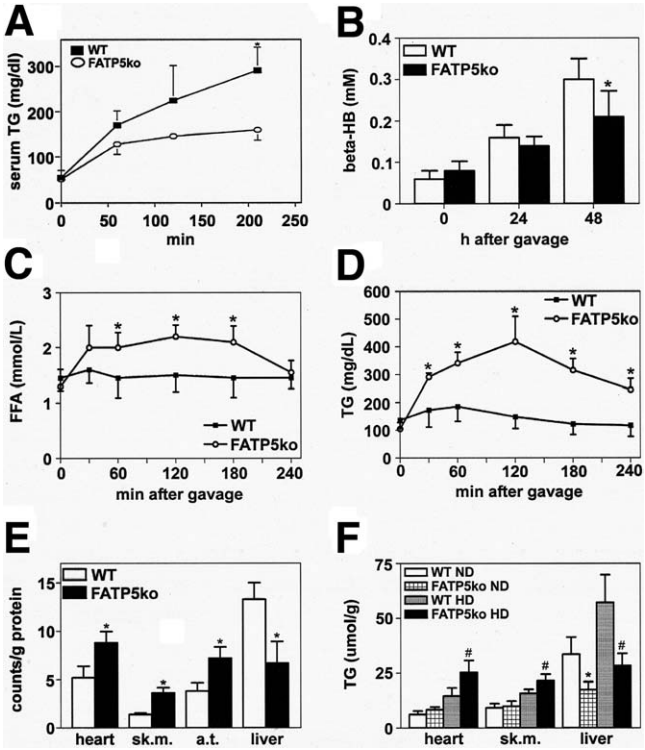

Figure 6. Measurement of hepatic metabolite output in the fasting state and absorption and deposition in the postprandial state. (*A*) Hepatic TG secretion. Serum TG levels of fasted wild-type and FATP5 knockout mice was measured at the indicated points after intravenous injection of Triton WR 1339. Data represent means ± SEM from a representative experiment of 3 animals per group that was repeated 2 times. (*B*) β-Hydroxybutyrate, (*C*) serum FFA, and (*D*) TG levels were determined in overnight-fasted FATP5 knockout and wild-type animals followed by an oil gavage at the indicated time points. Graphs represent means ± SEM of data from 3 independent experiments, each assayed in triplicate. (*E*) Distribution of radioactivity in organs of FATP5 knockout and wild-type animals 4 hours after intragastric administration of an olive oil bolus containing ^{14}C–oleic acid tracer. Error bars indicate ±SEM of 5 representative measurements. sk.m., skeletal muscle; a.t., adipose tissue. (*F*) TG content in tissues from FATP5 knockout and wild-type animals on normal diet (ND) and after a 12-week high-fat challenge (HD). (*A–F*) $^{*}P < .05$ in *t* test between wild-type and FATP5 knockout animals (normal chow). (*F*) $^{\#}P < .05$ in *t* test between wild-type and FATP5 knockout animals (high-fat diet).

Loss of FATP5 Causes a Redistribution of Dietary Lipids From the Liver to Other FFA-Metabolizing Tissues

To assess changes in the tissue distribution of dietary lipids due to the reduced hepatic uptake, we performed oil gavages containing ^{14}C-oleate tracer after an overnight fast and measured the amount of ^{14}C radioactivity in several organs. As shown in Figure 6*E*, in our experiments we could demonstrate a postprandial redistribution of dietary fats away from the liver to other FFA-metabolizing tissues, such as skeletal and cardiac muscle, and adipose tissue, which do not express liver-specific FATP5 but other members of the FATP family.[13,16,18,21,45] As expected from the FATP5 deletion, postgavage levels of ^{14}C-oleate tracer in liver were significantly decreased (Figure 6*E*). These results are in line with our findings that chronic loss of FATP5 function leads to a redistribution of lipids among organs at the end of a 12-week high-fat diet challenge (60% caloric fat content, D12492; Research Diets, New Brunswick, NJ) compared with animals fed with normal chow (Figure 6*F*). In summary, our data clearly indicate that loss of FATP5 alters regulation of hepatic lipid uptake and output while causing a redistribution of lipids away from the liver to other tissues.

FATP5 Deletion Affects Several Serum Metabolites

The alterations in hepatic lipid metabolism found in the FATP5 knockout mice significantly affected the levels of several serum metabolites. Serum TG, FFA, and cholesterol concentrations were significantly reduced in the FATP5 knockout animals compared with the wild-type littermates (Table 1). Interestingly, we found that FATP5 knockout mice had significantly increased serum glucose levels and showed a trend toward elevated insulin levels (Table 1). Basic liver function, however, seemed unaffected by FATP5 deficiency, as serum albumin, alanine aminotransferase, and bilirubin levels were generally comparable to that in wild-type animals (Table 1).

Discussion

The liver has long been believed to have an active, protein-mediated mechanism for the uptake of LCFAs.[9] However, the identity of the presumed hepatic FA transporter has remained controversial. Possible candidates include FAT/CD36,[19,20] FABPpm, and FATPs (Slc27 family).[21,25] FABPpm was later found to be identical to mitochondrial aspartate aminotransferase (mAspAT), an enzyme used to catalyze transamination reactions that link urea metabolism and the Krebs cycle,[46] and it remains unclear how a bona fide mitochondrial protein could enhance LCFA uptake at the membrane. While there is good evidence that CD36 enhances LCFA uptake, it is only expressed at low levels in the liver, and CD36-null animals show an increased, rather than reduced, liver TG content.[22–24]

Two members of the FATP family, FATP2 (Slc27a2) and FATP5 (Slc27a5), have been found to be strongly expressed in the liver.[21] Based on sequence similarities, FATP5 is a member of the FATP/Slc27 protein family.[21] Overexpression of FATP5 causes an increase in FA uptake, using the fluorescently labeled LCFA analogue C1-

Table 1. Body Weights and Serum Parameters of FATP5 Knockout and Wild-Type Mice on Normal Chow Ad Libitum

Parameter	Wild-type mice	Knockout mice	*P* value
Body wt (*g*)	29.8 ± 2.24	29.6 ± 0.65	NS
Glucose (*mg/dL*)	92 ± 12.8	114 ± 11.6	.009
Insulin (*ng/mL*)	0.76 ± 0.15	0.95 ± 0.13	.048
FFA (*nmol/L*)	1.59 ± 0.07	1.39 ± 0.03	.0001
TG (*mg/dL*)	126 ± 12.8	104 ± 7.36	.005
Cholesterol (*mmol/L*)	7.5 ± 1.3	4.8 ± 1.5	.045
β-hydroxybuturate (*mg/dL*)	9.70 ± 1.58	7.69 ± 2.0	NS
Alanine aminotransferase (*U/L*)	33.2 ± 2.54	31.8 ± 3.09	NS
Albumin (*g/dL*)	2.2 ± 0.44	2.3 ± 0.52	NS
Bilirubin (*mg/dL*)	1.082 ± 0.17	0.985 ± 0.26	NS

NOTE. Parameters are from overnight fasted animals 8–12 weeks of age (n = 5–6).

BODIPY-C12,[21] and has also been reported to increase long-chain and very-long-chain acyl-CoA synthetase[28] as well as bile acid/CoA synthetase[29,30] activities. Here we report that, based on RNA and protein detection methods, FATP5 is indeed a liver-specific protein that is primarily expressed by hepatocytes where it localizes to the basal membrane. Immunofluorescent and immunoelectron localization of FATP5 protein in liver sections revealed a preferred localization to the space of Disse, and its expression follows closely the hepatic microvasculature. Targeting of FATP5 to the hepatocyte/sinusoidal interface is congruent with a role in serum FA uptake and the reconjugation of bile acids from the enterohepatic circulation. While we could show that FATP5 clearly enhances the uptake of oleate and also acts as a bile-CoA ligase (Hubbard et al[31]), we could demonstrate that it does not function as a general bile transporter like the SLC10 family members.[47] However, because unconjugated bile acids can enter cells without a bile transporter,[48] FATP5 may increase their intracellular concentration by metabolic trapping.

Interestingly and similar to FATP5, a targeting to membrane areas juxtaposed to microvasculature has also been shown for the heart-specific FATP6.[37] Our in vivo localization data are in contrast to earlier reports of *myc*-tagged FATP5 protein being predominantly localized to the endoplasmic reticulum of transiently transfected COS cells.[29] It is important to note that our studies were performed with primary tissues and cells, thus eliminating possible artifacts due to the presence of protein tags or as a result of overexpression.

Loss of FATP5 significantly impacted hepatic lipid metabolism. In line with a postulated role of FATP5 in LCFA uptake, FATP5 knockout hepatocytes showed a 50% reduced uptake of both fluorescently and radioactively labeled LCFAs. It is unlikely that the remaining uptake activity is due to passive diffusion because 90% of the total hepatic LCFA uptake is due to a saturable process.[11] Our Western blot analyses showed that both wild-type and FATP5 knockout livers express significant amounts of FATP2 and, to a lesser degree, FATP3. We therefore speculate that the FATP5-independent hepatic LCFA uptake is largely due to other members of the FATP family such as FATP2. A targeted deletion of the *FATP2* gene in mice has recently been described[45]; however, its effect on FA uptake has not been examined.

The significantly reduced LCFA uptake by FATP5 knockout hepatocytes provides the first in vivo evidence that cell surface proteins, such as FATPs, contribute substantially to this process in the liver. Similarly, other in vivo studies have shown the importance of FATP4 and FATP1 for LCFA uptake by the intestine[37] and skeletal muscle,[49] highlighting the general importance of this protein family for FA uptake and metabolism.

While our in vitro data clearly show that overexpression of FATP5 alone results in an increased LCFA uptake in cultured mammalian cells, it is likely that its function is closely associated with other upstream- as well as downstream-located transporters, binding proteins, or acyl-CoA synthetases ensuring efficient LCFA uptake. Further, while FATP5 has been shown to possess very-long-chain acyl-CoA synthetase activity,[28] it remains to be determined whether additional plasma membrane acyl-CoA synthetases are required for efficient hepatic LCFA uptake. Potential candidates for interactions include CD36,[19,20] FABP,[19,20] LACS,[50] and possibly FATP2.[18,45] Although a deeper biochemical and structural understanding of FATP-mediated LCFA uptake awaits further investigation, our data presented in this report clearly show that FATP5 is both required and sufficient for an efficient hepatic LCFA uptake.

As would be expected from a reduced hepatic LCFA uptake, liver FFA, cholesterol ester, diglyceride, and TG levels were all significantly lower in FATP5 knockout animals. There were no significant effects on the distribution of acyl chain lengths and we did not observe any signs of perturbed very long-chain fatty acid metabolism, which would argue that FATP5 very-long-chain acyl-CoA synthetase activity plays only a minor role in vivo. Interestingly, loss of FATP5 protein impacted liver TG levels more than any other FA transport compartment. Taken together with the finding that overexpression of FATP1 has been linked to a preferential increase in TG levels,[51] this could indicate a predominant channeling of FAs by FATPs toward TG synthesis and storage rather than mitochondrial import and β-oxidation.

We also observed a disproportionately large effect of FATP5 deletion on saturated FAs compared with monounsaturated and polyunsaturated FAs. The percentage of 16:0 FAs was decreased in liver TGs and FFAs, whereas the percentage of 18:1n9 was higher in the FATP5 knockout mice. These observations are consistent with a decreased uptake of dietary FAs and an increased de novo synthesis of preferentially monounsaturated LCFAs to compensate for the disturbed LCFA supply from the diet. This hypothesis is supported by the increased concentration of neutral lipids in FATP5 knockout livers in zone 3 of hepatic lobules and by the increased FAS expression and increased cerulenin susceptibility. Alternatively, FATP5 may have a higher affinity for saturated FAs compared with the postulated additional liver LCFA transporter(s).

Interestingly, hepatic levels of phospholipids, particularly phosphatidylserine, were increased in FATP5 knockout livers. Phosphatidylserine is a critical membrane phospholipid and can be as much as 10% of the cellular phospholipids. It is normally restricted to the inner leaflet of the plasma membrane and participates, in addition to its structural functions, in multiple cellular signaling pathways.[52] Additionally, the FA composition of another phospholipid, phosphatidylcholine, was significantly different between FATP5 knockout and wild-type mice. Phosphatidylcholine is the most abundant phospholipid in mammalian cells. Like phosphatidylserine, phosphatidylcholine has important structural properties for the cell. Here as well, the monounsaturated FA content in phosphatidylcholine was increased in the knockout mice while the saturated FA content was decreased. Similar to the effect of FATP5 deletion on hepatic FA composition, this shift was characterized primarily by a change in n-9 FAs, that is, the relative concentration of 18:1n9 was significantly increased, which may be due to the increased levels of 18:1n9 FAs in the liver being shunted into the production of phosphatidylcholine. Although the direct consequences of the alterations in phospholipid level and composition are unknown, these findings could possibly be linked to the observed hepatomegaly in the FATP5 knockout animals, as described in our companion report (Hubbard et al[31]). While we cannot exclude the possibility that the decrease in hepatic lipid content is connected to alterations in bile metabolism, it is more likely a result of decreased LCFA uptake from the circulation because FATP5 knockout animals showed no malabsorption of lipids when fed a high-fat diet (Hubbard et al[31]).

We also observed that the changes in hepatic lipid homeostasis in FATP5 knockout animals were reflected by profound alterations in serum metabolites (this report and Hubbard et al[31]). In the FATP5 knockout animals, FFA, TG, and cholesterol levels were significantly reduced under fasting conditions. This decrease is likely a direct result of the reduced liver lipid stores leading to the observed decrease in hepatic very-low-density lipoprotein output. Interestingly, in FATP5 knockout mice fed on normal chow, we observed significantly increased serum glucose levels and a slight trend toward hyperinsulinemia. This finding differs from our observations made on a high-fat diet (Hubbard et al[31]). Similar, albeit more pronounced, changes in serum TG, glucose, and insulin levels were found in the LIRKO mouse model.[53] However, our finding was unexpected because decreased hepatocellular FFA levels, as found in FATP5 knockout mice, should rather improve hepatic insulin sensing and decrease glucose production.[54]

Further, as a likely result of the depletion of liver lipid stores, we also found severe alterations in metabolite absorption and clearance in FATP5 knockout mice. The ketogenetic response was severely impaired after FATP5 deletion during a 48-hour fasting period as assessed by the formation of β-hydroxybutyrate. Conversely, postabsorptive lipid clearance was severely diminished in FATP5 knockout mice, as would be expected from an impaired hepatic FFA uptake as a result of the FATP5 deletion. While FATP5 knockout mouse livers are overall enlarged and show a 25% increase in hepatocyte size compared with livers of wild-type animals, no evidence of fibrosis or other structural disorders in the FATP5 knockout mouse livers was found. Furthermore, serum alanine aminotransferase, albumin, and bilirubin levels were similar between FATP5 knockout and wild-type mice, again pointing to an unimpaired basic liver function. Moreover, in our accompanying report, we could show comparable values of the respiratory exchange ratios and of expression levels of FA oxidation markers (Hubbard et al[31]), which as well should exclude a major hepatic dysfunction in the FATP5 knockout mouse model.

Taken together, our data describing the FATP5 knockout mouse show a significant reduction in both liver lipid uptake and content. On the other hand, we could demonstrate a decrease in the concentrations of diverse serum lipids. Besides these findings, our investigations point to an unaltered intestinal lipid absorption. To link these findings and to also address the observed trend toward a hyperglycemic/hyperinsulinemic phenotype, we performed oil gavages containing ^{14}C-oleate tracer. The results gained from these experiments reveal a redistribution of dietary fats in the postprandial state away from the liver toward tissues whose uptake is dominated by other members of the FATP family, such as skeletal and cardiac muscle. This in turn could lead to insulin desensitization and a decreased glucose uptake and utilization by these tissues followed by an elevated

serum insulin concentration. These findings are also consistent with our observations that both hearts from FATP5-null mice are enlarged (data not shown) and chronic loss of FATP5 function leads to a redistribution of lipids among organs at the end of a 12-week high-fat diet challenge. Moreover, in line with our hypothesis, that the partial FFA uptake defect in liver may result in an increased availability of FFAs to other tissues, would also be our observation of an increased thermogenesis, potentially as a consequence of an increased availability of FFAs to muscle and brown adipocytes (Hubbard et al[31]). It is noteworthy that higher insulin levels also promote the transcription of SREBP, a key regulator of nutritional homeostasis and insulin action, which in addition could contribute to increased serum glucose levels due to the stimulation of hepatic glycolytic enzymes.[55,56] Lastly, and linking back to the serum FA levels, the observed higher insulin concentrations in the FATP5 knockout mice could result in a suppression of lipolysis in adipocytes leading to a decreased FFA output,[57–59] which would also add to a reduced serum lipid concentration as described previously. Additional studies, including euglycemic/hyperinsulinemic clamp experiments, are under way to further investigate these findings in more detail.

In conclusion, our studies shown here and in the accompanying report by Hubbard et al[31] suggest that FATP5 is a protein with multiple activities and can contribute to both bile acid reactivation and hepatic FA uptake and lipid accumulation. These findings begin to shed light on the complex interrelationships in hepatic lipid biology and should further our understanding of metabolic disorders, such as nonalcoholic fatty liver disease, diet-induced obesity, and type 2 diabetes mellitus.

References

1. Odaib AA, Shneider BL, Bennett MJ, Pober BR, Reyes-Mugica M, Friedman AL, Suchy FJ, Rinaldo P. A defect in the transport of long-chain fatty acids associated with acute liver failure. N Engl J Med 1998;339:1752–1757.
2. Rinaldo P. Fatty acid transport and mitochondrial oxidation disorders. Semin Liver Dis 2001;21:489–500.
3. Masuzaki H, Paterson J, Shinyama H, Morton NM, Mullins JJ, Seckl JR, Flier JS. A transgenic model of visceral obesity and the metabolic syndrome. Science 2001;294:2166–2170.
4. Saltiel AR, Kahn CR. Insulin signalling and the regulation of glucose and lipid metabolism. Nature 2001;414:799–806.
5. Marchesini G, Brizi M, Bianchi G, Tomassetti S, Bugianesi E, Lenzi M, McCullough AJ, Natale S, Forlani G, Melchionda N. Nonalcoholic fatty liver disease: a feature of the metabolic syndrome. Diabetes 2001;50:1844–1850.
6. Elsing C, Winn-Borner U, Stremmel W. Confocal analysis of hepatocellular long-chain fatty acid uptake. Am J Physiol 1995;269: G842–G851.
7. Fitscher B, Klaassen-Schluter C, Stremmel W. Evidence for a hepatocyte membrane fatty acid transport protein using rat liver mRNA expression in Xenopus laevis oocytes. Biochim Biophys Acta 1995;1256:47–51.
8. Sorrentino D, Stump DD, Van Ness K, Simard A, Schwab AJ, Zhou SL, Goresky CA, Berk PD. Oleate uptake by isolated hepatocytes and the perfused rat liver is competitively inhibited by palmitate. Am J Physiol 1996;270:G385–G392.
9. Stremmel W. Mechanism of hepatic fatty acid uptake. J Hepatol 1989;9:374–382.
10. Stremmel W. Transmembrane transport of fatty acids in the heart. Mol Cell Biochem 1989;88:23–29.
11. Stump DD, Nunes RM, Sorrentino D, Isola LM, Berk PD. Characteristics of oleate binding to liver plasma membranes and its uptake by isolated hepatocytes. J Hepatol 1992;16:304–315.
12. Gore J, Hoinard C. Linolenic acid transport in hamster intestinal cells is carrier-mediated. J Nutr 1993;123:66–73.
13. Stahl A, Hirsch DJ, Gimeno R, Punreddy S, Ge P, Watson N, Kotler M, Tartaglia LA, Lodish HF. Identification of a small intestinal fatty acid transport protein. Mol Cell 1999;4:299–308.
14. Stremmel W. Uptake of fatty acids by jejunal mucosal cells is mediated by a fatty acid binding membrane protein. J Clin Invest 1988;82:2001–2010.
15. Sorrentino D, Stump D, Potter BJ, Robinson RB, White R, Kiang CL, Berk PD. Oleate uptake by cardiac myocytes is carrier mediated and involves a 40-kD plasma membrane fatty acid binding protein similar to that in liver, adipose tissue, and gut. J Clin Invest 1988;82:928–935.
16. Schaffer JE, Lodish HF. Expression cloning and characterization of a novel adipocyte long chain fatty acid transport protein. Cell 1994;79:427–436.
17. Abumrad N, Harmon C, Ibrahimi A. Membrane transport of long-chain fatty acids: evidence for a facilitated process. J Lipid Res 1998;39:2309–2318.
18. Stahl A, Gimeno RE, Tartaglia LA, Lodish HF. Fatty acid transport proteins: a current view of a growing family. Trends Endocrinol Metab 2001;12:266–273.
19. Abumrad N, Coburn C, Ibrahimi A. Membrane proteins implicated in long-chain fatty acid uptake by mammalian cells: CD36, FATP and FABPm. Biochim Biophys Acta 1999;1441:4–13.
20. Ibrahimi A, Abumrad NA. Role of CD36 in membrane transport of long-chain fatty acids. Curr Opin Clin Nutr Metab Care 2002;5: 139–145.
21. Hirsch D, Stahl A, Lodish HF. A family of fatty acid transporters conserved from mycobacterium to man. Proc Natl Acad Sci U S A 1998;95:8625–8629.
22. Coburn CT, Hajri T, Ibrahimi A, Abumrad NA. Role of CD36 in membrane transport and utilization of long-chain fatty acids by different tissues. J Mol Neurosci 2001;16:117–121; discussion 151–157.
23. Coburn CT, Knapp FF Jr, Febbraio M, Beets AL, Silverstein RL, Abumrad NA. Defective uptake and utilization of long chain fatty acids in muscle and adipose tissues of CD36 knockout mice. J Biol Chem 2000;275:32523–32529.
24. Febbraio M, Abumrad NA, Hajjar DP, Sharma K, Cheng W, Pearce SF, Silverstein RL. A null mutation in murine CD36 reveals an important role in fatty acid and lipoprotein metabolism. J Biol Chem 1999;274:19055–19062.
25. Berger J, Truppe C, Neumann H, Forss-Petter S. A novel relative of the very-long-chain acyl-CoA synthetase and fatty acid transporter protein genes with a distinct expression pattern. Biochem Biophys Res Commun 1998;247:255–260.
26. Coe N, Smith A, Frohnert B, Watkins P, Bernlohr D. The fatty acid transport protein (FATP1) is a very long chain acyl-CoA synthetase. J Biol Chem 1999;274:36300–36304.
27. Fitscher BA, Riedel HD, Young KC, Stremmel W. Tissue distribution and cDNA cloning of a human fatty acid transport protein (hsFATP4). Biochim Biophys Acta 1998;1443:381–385.

28. Steinberg SJ, Kemp S, Braiterman LT, Watkins PA. Role of very-long-chain acyl-coenzyme A synthetase in X-linked adrenoleukodystrophy. Ann Neurol 1999;46:409–412.
29. Mihalik SJ, Steinberg SJ, Pei Z, Park J, Kim DG, Heinzer AK, Dacremont G, Wanders RJ, Cuebas DA, Smith KD, Watkins PA. Participation of two members of the very long-chain acyl-CoA synthetase family in bile acid synthesis and recycling. J Biol Chem 2002;277:24771–24779.
30. Steinberg SJ, Mihalik SJ, Kim DG, Cuebas DA, Watkins PA. The human liver-specific homolog of very long-chain acyl-CoA synthetase is cholate:CoA ligase. J Biol Chem 2000;275:15605–15608.
31. Hubbard B, Doege H, Punreddy S, Wu H, Huang X, Kaushik V, Mozell RL, Byrnes JJ, Stricker-Krongrad A, Chou J, Tartaglia LA, Lodish HF, Stahl A, Gimeno RE. Mice deleted for fatty acid transport protein 5 have defective bile acid conjugation and are protected from obesity. Gastroenterology 2006;130:1259–1269.
32. Millar JS, Maugeais C, Fuki IV, Rader DJ. Normal production rate of apolipoprotein B in LDL receptor-deficient mice. Arterioscler Thromb Vasc Biol 2002;22:989–994.
33. Nilsson-Ehle P, Schotz MC. A stable, radioactive substrate emulsion for assay of lipoprotein lipase. J Lipid Res 1976;17:536–541.
34. Folch J, Lees M, Sloane Stanley GH. A simple method for the isolation and purification of total lipides from animal tissues. J Biol Chem 1957;226:497–509.
35. Stremmel W, Berk PD. Hepatocellular influx of [14C]oleate reflects membrane transport rather than intracellular metabolism or binding. Proc Natl Acad Sci U S A 1986;83:3086–3090.
36. Stremmel W, Strohmeyer G, Berk PD. Hepatocellular uptake of oleate is energy dependent, sodium linked, and inhibited by an antibody to a hepatocyte plasma membrane fatty acid binding protein. Proc Natl Acad Sci U S A 1986;83:3584–3588.
37. Gimeno RE, Ortegon AM, Patel S, Punreddy S, Ge P, Sun Y, Lodish HF, Stahl A. Characterization of a heart-specific fatty acid transport protein. J Biol Chem 2003;278:16039–16044.
38. Watkins SM, Reifsnyder PR, Pan HJ, German JB, Leiter EH. Lipid metabolome-wide effects of the PPARgamma agonist rosiglitazone. J Lipid Res. 2002;43:1809–1817.
39. Frachon S, Gouysse G, Dumortier J, Couvelard A, Nejjari M, Mion F, Berger F, Paliard P, Boillot O, Scoazec JY. Endothelial cell marker expression in dysplastic lesions of the liver: an immunohistochemical study. J Hepatol 2001;34:850–857.
40. Hagenbuch B, Dawson P. The sodium bile salt cotransport family SLC10. Pflugers Arch 2004;447:566–570.
41. Hagenbuch B, Stieger B, Foguet M, Lubbert H, Meier PJ. Functional expression cloning and characterization of the hepatocyte Na+/bile acid cotransport system. Proc Natl Acad Sci U S A 1991;88:10629–10633.
42. Jungermann K. Role of intralobular compartmentation in hepatic metabolism. Diabete Metab 1992;18:81–86.
43. Hirsch J. The search for new ways to treat obesity. Proc Natl Acad Sci U S A 2002;99:9096–9097.
44. Loftus TM, Jaworsky DE, Frehywot GL, Townsend CA, Ronnett GV, Lane MD, Kuhajda FP. Reduced food intake and body weight in mice treated with fatty acid synthase inhibitors. Science 2000; 288:2379–2381.
45. Heinzer AK, Watkins PA, Lu JF, Kemp S, Moser AB, Li YY, Mihalik S, Powers JM, Smith KD. A very long-chain acyl-CoA synthetase-deficient mouse and its relevance to X-linked adrenoleukodystrophy. Hum Mol Genet 2003;12:1145–1154.
46. Berk PD, Wada H, Horio Y, Potter BJ, Sorrentino D, Zhou SL, Isola LM, Stump D, Kiang CL, Thung S. Plasma membrane fatty acid-binding protein and mitochondrial glutamic-oxaloacetic transaminase of rat liver are related. Proc Natl Acad Sci U S A 1990;87: 3484–3488.
47. Stremmel W. Translocation of fatty acids across the basolateral rat liver plasma membrane is driven by an active potential-sensitive sodium-dependent transport system. J Biol Chem 1987;262:6284–6289.
48. Parks DJ, Blanchard SG, Bledsoe RK, Chandra G, Consler TG, Kliewer SA, Stimmel JB, Willson TM, Zavacki AM, Moore DD, Lehmann JM. Bile acids: natural ligands for an orphan nuclear receptor. Science 1999;284:1365–1368.
49. Kim JK, Gimeno RE, Higashimori T, Kim HJ, Choi H, Punreddy S, Mozell RL, Tan G, Stricker-Krongrad A, Hirsch DJ, Fillmore JJ, Liu ZX, Dong J, Cline G, Stahl A, Lodish HF, Shulman GI. Inactivation of fatty acid transport protein 1 prevents fat-induced insulin resistance in skeletal muscle. J Clin Invest 2004;113:756–763.
50. Suzuki H, Kawarabayasi Y, Kondo J, Abe T, Nishikawa K, Kimura S, Hashimoto T, Yamamoto T. Structure and regulation of rat long-chain acyl-CoA synthetase. J Biol Chem 1990;265:8681–8685.
51. Hatch GM, Smith AJ, Xu FY, Hall AM, Bernlohr DA. FATP1 channels exogenous FA into 1,2,3-triacyl-sn-glycerol and down-regulates sphingomyelin and cholesterol metabolism in growing 293 cells. J Lipid Res 2002;43:1380–1389.
52. Vance JE. Molecular and cell biology of phosphatidylserine and phosphatidylethanolamine metabolism. Prog Nucleic Acid Res Mol Biol 2003;75:69–111.
53. Michael MD, Kulkarni RN, Postic C, Previs SF, Shulman GI, Magnuson MA, Kahn CR. Loss of insulin signaling in hepatocytes leads to severe insulin resistance and progressive hepatic dysfunction. Mol Cell 2000;6:87–97.
54. Lam TK, van de Werve G, Giacca A. Free fatty acids increase basal hepatic glucose production and induce hepatic insulin resistance at different sites. Am J Physiol Endocrinol Metab 2003;284:E281–E290.
55. Foretz M, Pacot C, Dugail I, Lemarchand P, Guichard C, Le Liepvre X, Berthelier-Lubrano C, Spiegelman B, Kim JB, Ferre P, Foufelle F. ADD1/SREBP-1c is required in the activation of hepatic lipogenic gene expression by glucose. Mol Cell Biol 1999;19:3760–3768.
56. Kim JB, Spiegelman BM. ADD1/SREBP1 promotes adipocyte differentiation and gene expression linked to fatty acid metabolism. Genes Dev 1996;10:1096–1107.
57. Rebrin K, Steil GM, Getty L, Bergman RN. Free fatty acid as a link in the regulation of hepatic glucose output by peripheral insulin. Diabetes 1995;44:1038–1045.
58. Rebrin K, Steil GM, Mittelman SD, Bergman RN. Causal linkage between insulin suppression of lipolysis and suppression of liver glucose output in dogs. J Clin Invest 1996;98:741–749.
59. Lewis GF, Vranic M, Harley P, Giacca A. Fatty acids mediate the acute extrahepatic effects of insulin on hepatic glucose production in humans. Diabetes 1997;46:1111–1119.

Received September 12, 2005. Accepted December 14, 2005.

Address requests for reprints to: Andreas Stahl, PhD, Palo Alto Medical Foundation Research Institute, Ames Building, 795 El Camino Real, Palo Alto, California 94301. e-mail: astahl@stanford.edu.

Supported by a training and feasibility grant from the Stanford Digestive Disease Center (National Institutes of Health grant DK56339), a grant from the National Institute of Diabetes and Digestive and Kidney Disease (National Institutes of Health grant DK066336-01 to A.S.), and in part by a grant from the National Institutes of Health (National Institutes of Health/National Heart, Lung, and Blood Institute grant PO1 HL66105 to Dr Harvey F. Lodish at the Whitehead Institute for Biomedical Research).

The authors thank Jon Mulholland and Kitty Lee at the Stanford Cell Science Imaging Facility for expert advice and help with light microscopy; Ann Strauss, Victoria Fairchild-Huntress, and Dennis Huszar for help with knockout generation; Dr Harvey F. Lodish for his contribution in creating FATP5 knockout animals; Dr Sung-Shin Choi for assistance with lipase assays; BD Bioscience for providing us with controls for Northern blots; the Palo Alto Medical Foundation Research Institute animal facility staff for their help; and Rosemary Grammer for critical reading of the manuscript.